Entropy **2015**, *17*, 5257-5273; doi:10.3390/e17085257

OPEN ACCESS

entropy

ISSN 1099-4300

www.mdpi.com/journal/entropy

Article

A Pilot Directional Protection for HVDC Transmission Line Based on Relative Entropy of Wavelet Energy

Sheng Lin *, Shan Gao, Zhengyou He and Yujia Deng

School of Electrical Engineering, Southwest Jiaotong University, Chengdu 610031, China;
E-Mails: togaoshan@outlook.com (S.G.); hezy@swjtu.edu.cn (Z.H.); dyj491505@163.com (Y.D.)

* Author to whom correspondence should be addressed; E-Mail: slin@swjtu.cn;
Fax: +86-28-8760-5114.

Academic Editor: Raúl Alcaraz Martínez

Received: 29 May 2015 / Accepted: 20 July 2015 / Published: 27 July 2015

Abstract: On the basis of analyzing high-voltage direct current (HVDC) transmission system and its fault superimposed circuit, the direction of the fault components of the voltage and the current measured at one end of transmission line is certified to be different for internal faults and external faults. As an estimate of the differences between two signals, relative entropy is an effective parameter for recognizing transient signals in HVDC transmission lines. In this paper, the relative entropy of wavelet energy is applied to distinguish internal fault from external fault. For internal faults, the directions of fault components of voltage and current are opposite at the two ends of the transmission line, indicating a huge difference of wavelet energy relative entropy; for external faults, the directions are identical, indicating a small difference. The simulation results based on PSCAD/EMTDC show that the proposed pilot protection system acts accurately for faults under different conditions, and its performance is not affected by fault type, fault location, fault resistance and noise.

Keywords: wavelet transform; relative entropy of wavelet energy; HVDC transmission system; direction feature; fault components of voltage and current; pilot protection

---

1. Introduction

High-voltage direct-current (HVDC) transmission systems have been widely applied to power transmission projects with long overhead transmission lines, bulk power and asynchronous interconnections because of their lower-cost transmission lines and larger power transmission capability [1,2]. However, their remote distance, complex surroundings and unpredictable weather conditions lead to a high failure rate, which requires protection methods with high reliability, fast response ability and sufficient sensitivity. There exist several problems in the current commonly used protection methods, including traveling-wave protection, dc minimum voltage protection and dc differential protection [3]. That is, if a fault is not properly detected or removed, it might cause widespread damage or a power system blackout [4]. Aiming to preserve the stability and reliability of HVDC transmission systems, it is crucial to find new protection principles for further study.

Based on the characteristics of the reactor-filter unit, which is made of a smoothing reactor and dc-side filter, the absolute-value integration of one-end current signals in some particular frequency bands were used to formulate the protection criteria [1]. However, high-resistance grounding leads to a fairly small current so that the current in characteristic frequency bands might be smaller than the setting value when a fault occurs. Therefore a protection system using one-end current would fail to operate. By this reason, in [5], according to the comparison of the energy of the forward and backward voltage traveling wave, the fault position can be recognized. Moreover, a pilot directional protection scheme for HVDC transmission line is proposed, which extracts the direction feature of specific frequency current through spectrum analysis and integral [6,7]. However, these methods don't have strong robustness to noise because the integral cannot get rid of noise disturbance and the fault current energy would be low and the integral would be much smaller when a high-resistance fault occurs.

To improve the reliability of the protection algorithms, signal processing was introduced into transmission line protection. For instance, in [8] Wavelet Transform (WT) has been applied to extract transient characteristics of different fault conditions for analyzing various transient voltage traveling waves. WT has the function of filtering, which can get rid of noise disturbance [9]. In [10], a technique similar to Discrete Fourier Transform (DFT) is presented for decomposing the transient components of current signals. Due to the effectiveness of WT in transient analysis, this technique has been combined with other techniques with the aim of improving the reliability of protection schemes. In [11–13], Shannon entropy is combined with WT which acts as an automatic feature extractor for distinguishing stable and unstable power swings. In other words, wavelet entropy can identify the power signals with different complexity. Therefore, in [14,15] the wavelet singular entropy is applied to describe the signals with different complexity which can distinguish internal fault from external fault. Moreover, wavelet energy entropy has a unique sensibility to slight change of signals and it can reflect the energy distribution information in both time and frequency domain [16,17]. In [18], relative entropy is considered to be a measure of the normal signals and the faulty signals, which can discriminate between the faulty groups and the normal groups.

In this paper, a novel algorithm for transmission line protection is proposed following the principle of relative entropy of wavelet energy, having improved the reliability of protection method proposed in [7] under high resistance grounding fault conditions and its anti-noise property. Furthermore, the proposal is based on the analysis of the HVDC transmission system and its superimposed circuit which indicate

the directional features of the voltage and current. The results are discussed with the aim to assess the advantages of the proposed algorithm and its reliability under different fault conditions. The proposed protection method can recognize internal faults correctly and quickly.

2. Theoretical Background

2.1. Wavelet Transform

When a discrete signal $x(k)$ is wavelet transformed, it has high-frequency component coefficients $d_j(k)$ and low-frequency coefficient $a_j(k)$ at instant k and scale j. The frequency band ranges contained in the signal components $D_j(k)$ and $A_j(k)$ obtained by reconstruction are:

$$\begin{cases} D_j(k):[2^{-(j+1)}f_s, 2^{-j}f_s] \\ A_j(k):[0, 2^{-j}f_s] \end{cases} \tag{1}$$

where f_s is the sampling frequency, j = 1, 2, …, m. The original signal sequence $x(k)$ can be represented by the sum of all components, namely:

$$x(k) = D_1(k) + A_1(k) = D_1(k) + D_2(k) + A_2(k) = \sum_{j=1}^{m} D_j(k) + A_2(k) \tag{2}$$

Let $D_{m+1}(k) = A_m(k)$, we obtain:

$$x(k) = \sum_{j=1}^{m+1} D_j(k) \tag{3}$$

$D_j(k)$ represents the component of transient signal $x(k)$ at each scale. After orthogonal wavelet transform, energy of each scale can be obtained by squaring the reconstructed wavelet transform coefficients.

2.2. Wavelet Energy Entropy

Let $E = E_1, E_2, \cdots E_m$ be wavelet spectra of signal $x(k)$ at m scales. Then E is a partition of signal energy at scale domain. According to the characteristic of orthogonal wavelet transform, at a certain time window the total signal energy E is the sum of energy E_j of each component. If $p_j = E_j / E$, then $\sum_{j=1}^{m+1} p_j = 1$. We thus define wavelet energy entropy (WEE) as:

$$WEE = -\sum_{j=1}^{m+1} p_j \log p_j \tag{4}$$

From the above definition, the change law of WEE with time can be obtained as the window slides. The definition in Equation (4) reflects the energy distribution of voltage or current in frequency space. Since the wavelet function does not have pulse selection properties at either frequency domain or time domain but a support region, the partition of current or voltage energy at scale space indicates the energy distribution features in both time domain and frequency domain.

However, calculating the wavelet energy entropy of the voltage or current can only reflect the changes of one signal in the time-domain and frequency-domain instead of the relation between the two signals. Thus, wavelet energy entropy can indicate the presence of faults, but it can hardly discriminate internal faults from external faults. To analyze different directions of fault components, we need another tool which can compare two signals changing in the time and frequency scales.

2.3. Relative Entropy of Wavelet Energy

The energy of a signal $x_i(k)$ at scale j is $E_{ij} = \sum_{k=1}^{N} D_j^2(k)$ where k = 1, 2,…, N, and N is the length of signal $x_i(k)$. Then the sum of energy of all signals at j scale is:

$$E_j = \sum_{i=1}^{h} E_{ij} \tag{5}$$

where h represents the number of signals.

The proportion of energy of signal $x_i(k)$ in all of signals at j scale is:

$$p_{ij} = \frac{E_{ij}}{E_j} \tag{6}$$

and $\sum_{j=1}^{m+1} p_{ij} = 1$.

Similarly, the proportion of energy of signal $x_l(k)$ in all of the signals at j scale is p_{lj}. Define relative entropy of wavelet energy comparing signal $x_i(k)$ to signal $x_l(k)$ as:

$$\mathrm{M}_{il} = \sum_{j=1}^{m+1} \left| p_{ij} \ln \frac{p_{ij}}{p_{lj}} \right| \tag{7}$$

The relative entropy of wavelet energy comparing signal $x_l(k)$ to signal $x_i(k)$ is M_{li}. Therefore, relative entropy of wavelet energy between signal $x_i(k)$ and signal $x_l(k)$ is:

$$\mathrm{M} = \mathrm{M}_{il} + \mathrm{M}_{li} \tag{8}$$

The entropy computed by these sequences or coefficients reflect the spare degree of the coefficient matrix, *i.e.*, the order degree of the signal probability distribution. In addition, the distributions in wavelet phase space are different for various signals.

3. Fault Feature Analysis

Nowadays, most HVDC transmission projects are two-end bipolar DC transmission systems. Figure 1 shows the structure of a bipolar HVDC transmission system composed of converter transformers, converters, smoothing reactor, AC filter, DC filter and transmission line. Each converter unit is comprised of two 12-pulse converters in series. Protection equipment is installed on both sides of the transmission line, R and I are the positions where protection and measurement devices installed on the rectifier side and the invertor side respectively. 1 and 2 separately represent the positive pole and negative pole.

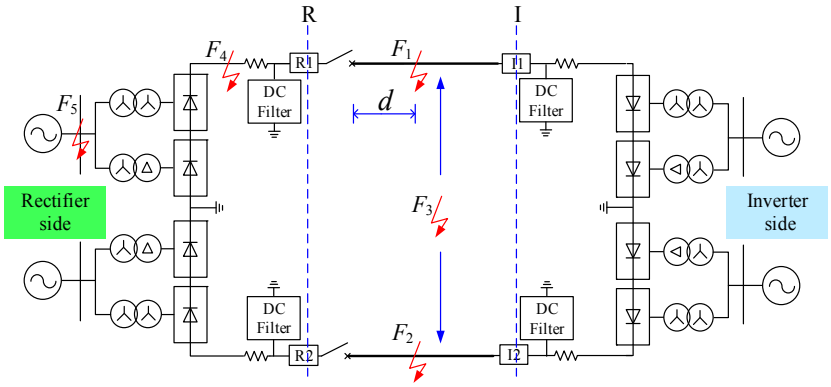

Figure 1. Bipolar HVDC transmission system structure.

According to the superposition principle, if a circuit has two or more independent sources, it can be analyzed by determining the contribution of each independent source to the variable and adding them up. Therefore, a fault state can be equivalent to the superposition of the normal state and an additional fault state. To simplify the HVDC transmission system, the AC side and converter station are equivalent to DC power supply while the smoothing filter and DC filter are equivalent to fixed impedance, which is represented by Z_F. Though the simplification cannot reflect the fault transient, it doesn't affect diagnosis using the characteristic of voltage and current. The line current and line voltage on each side of the simplified system when the HVDC transmission system operates normally are shown in Figure 2a,b. Z is the equivalent impedance of the transmission line. E_S is the voltage source of the equivalent model of AC system, while Z_S is the impedance of the equivalent model of AC system.

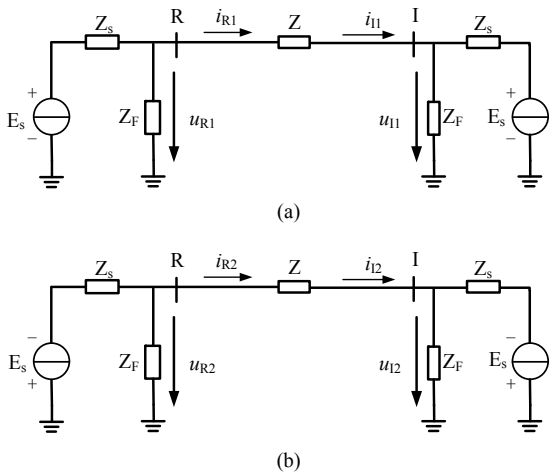

Figure 2. Simplified monopole HVDC transmission system without fault. (**a**) Simplified positive pole HVDC transmission system. (**b**) Simplified negative pole HVDC transmission system.

3.1. Internal Fault

When transmission lines have grounding faults (internal faults occurring in transmission lines), Figure 3a is the superimposed circuit for a positive line fault and Figure 3b is the superimposed circuit for a negative line fault. The simplified model of the positive pole and negative pole transmission line

can be analyzed independently, which is reckoned without the interaction of transmission lines after decoupling.

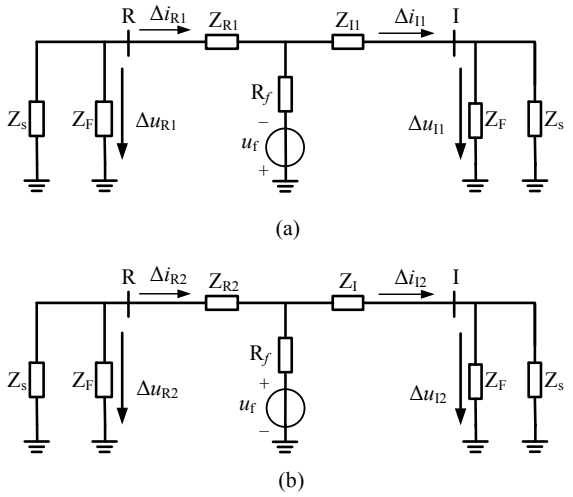

Figure 3. Fault superimposed circuit for an internal fault. (**a**) Simplified positive pole HVDC transmission system. (**b**) Simplified negative pole HVDC transmission system.

3.1.1. Positive Pole

An internal fault on a positive pole transmission line is equivalent to a negative voltage source at the fault position. Supposing that the voltage measured at the converter station doesn't change at transient analysis after a fault, then the superimposed circuit of positive pole transmission system is as shown in Figure 3a.

Since a grounding fault occurs in the middle of two boundaries of the positive transmission line, let Z_{R1} and Z_{I1} be the equivalent impedance of the transmission line close to the rectifier and inverter, respectively, and $Z_{R1}+Z_{I1}=Z$. R_f is the ground resistance while u_f represents the equivalent voltage source at the fault position. Δu_{R1}, Δu_{I1}, Δi_{R1} and Δi_{I1} are the voltage fault components and current fault components measured on each side of the positive pole transmission line. When a fault occurs on the positive pole transmission line:

$$\Delta u_{R1} = -(Z_S \parallel Z_F)\Delta i_{R1} \tag{9}$$

$$\Delta u_{I1} = (Z_S \parallel Z_F)\Delta i_{I1} \tag{10}$$

where the directions of Δu_{R1} and Δi_{R1} are opposite, while the directions of Δu_{I1} and Δi_{I1} are identical.

3.1.2. Negative Pole

The superimposed circuit of a negative pole transmission system is as shown in Figure 3b with a positive voltage source acting at the fault position.

In Figure 3b, similar to the positive pole, Δu_{R2}, Δu_{I2}, Δi_{R2} and Δi_{I2} are the voltage fault components and current fault components measured on each side of the negative pole transmission line. When a fault occurs on the negative pole transmission line:

$$\Delta u_{R2} = -(Z_S \parallel Z_F)\Delta i_{R2} \tag{11}$$

$$\Delta u_{I2} = (Z_S \parallel Z_F)\Delta i_{I2} \tag{12}$$

where the directions of Δu_{R2} and Δi_{R2} are opposite, while the directions of Δu_{I2} and Δi_{I2} are identical. If two transmission lines encounter a short circuit, the fault superimposed circuit of the positive pole and negative pole are shown as in Figure 3 after all. Thus, the directions of voltage fault components and current fault components on the rectifier-side are opposite while the directions on the inverter-side are identical.

3.2. External Fault

3.2.1. External Fault at the Rectifier-Side

When a fault occurs to a positive pole transmission system at the rectifier-side, the superimposed circuit is as shown by Figure 4.

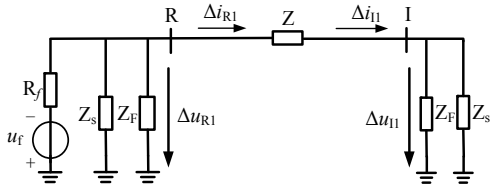

Figure 4. Fault superimposed circuit for an external fault at the rectifier-side on the positive pole.

The circuit in Figure 4 involves a dependent voltage source. To gain the relationship between current and voltage, applying KVL around the loop in Figure 4 gives:

$$\Delta u_{R1} = [Z + (Z_S \parallel Z_F)]\Delta i_{R1} \tag{13}$$

$$\Delta u_{I1} = (Z_S \parallel Z_F)\Delta i_{I1} \tag{14}$$

where the directions of Δu_{R1}, Δi_{R1} and the directions of Δu_{I1}, Δi_{I1} are all identical.

If a fault occurs to the negative pole transmission system at the rectifier-side, a similar superimposed circuit with positive pole transmission is shown as is Figure 4, except for the direction of u_f. Therefore, the relationship between voltage fault components and current fault components on both sides of transmission line is:

$$\Delta u_{R2} = [Z + (Z_S \parallel Z_F)]\Delta i_{R2} \tag{15}$$

$$\Delta u_{I2} = (Z_S \parallel Z_F)\Delta i_{I2} \tag{16}$$

where the directions of Δu_{R2}, Δi_{R2} and the directions of Δu_{I2}, Δi_{I2} are all identical.

Therefore, when an external fault occurs to a HVDC transmission system at the rectifier-side, the directions of the voltage fault components and current fault components on each side of transmission lines are identical.

3.2.2. External Fault at Inverter-Side

The superimposed circuit for an external fault at the inverter-side of a positive pole transmission system is as shown in Figure 5.

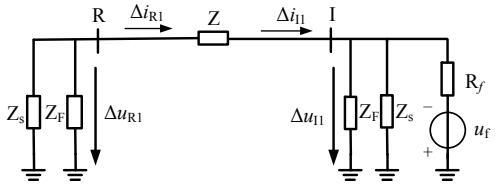

Figure 5. Fault superimposed circuit for an external fault at the inverter-side on the positive pole.

Applying KVL around the loop in Figure 5 gives:

$$\Delta u_{R1} = -(Z_S \| Z_F)\Delta i_{R1} \tag{17}$$

$$\Delta u_{I1} = -[Z + (Z_S \| Z_F)]\Delta i_{I1} \tag{18}$$

where the directions of Δu_{R1}, Δi_{R1} are opposite and the directions of Δu_{I1}, Δi_{I1} are also opposite.

Similarly, when an external fault occurs to a negative pole transmission system at the inverter-side, the fault components are calculated as below:

$$\Delta u_{R2} = -(Z_S \| Z_F)\Delta i_{R2} \tag{19}$$

$$\Delta u_{I2} = -[Z + (Z_S \| Z_F)]\Delta i_{I2} \tag{20}$$

where the directions of Δu_{R2}, Δi_{R2} are opposite and the directions of Δu_{I2}, Δi_{I2} are also opposite.

3.2. Summary

For internal fault, the directions of voltage and current fault components at the rectifier-side are opposite while the directions at the inverter-side are identical. However, for external faults, no matter whether at the rectifier-side or inverter-side, the relationship between the directions of voltage and current fault component are always the same, either opposite or identical. In this paper, we utilize wavelet entropy to extract the voltage and current information from a transmission line which can quantify the relationship between the directions of voltage and current fault components.

The wavelet entropy concept was generated by the generalization of information entropy in recent years. In this case, wavelet entropy not only solves the problem of refusal-operation under high resistance grounding fault conditions, but also avoids the influence of noise disturbance. The basic idea of wavelet entropy is to process the wavelet transform coefficients as a probability distribution sequence. Thus, the wavelet coefficients at each scale are regarded as the message of a signal source. We calculate the relative entropy of wavelet energy between the voltage fault component and current fault component to qualify their directions. Opposite direction corresponds to a large entropy while identical direction corresponds to a fairly small entropy.

4. Methods of Transmission Line Protection

4.1. Starting Criterion

According to the analysis in Section 3, the wavelet energy entropy of voltage or current would increase significantly when a fault occurs in a HVDC transmission system. Besides, current is more sensitive to short circuit failures. Hence, the wavelet energy entropy of current detected by a DC shunt is used as starting criterion, which is formulated as follows:

$$S_e > w \tag{21}$$

where S_e is the wavelet energy entropy of the measured current, calculated by Equation (4). w is the threshold that distinguishes grounding faults from disturbances. The selection principle of w is based on the calculation of the specific current detected during simulation of an external fault at the transmission line boundary. In addition, the sufficient reliability of the starting criterion should be taken into account. The protection startup scheme based on the current wavelet energy entropy is shown in Figure 6.

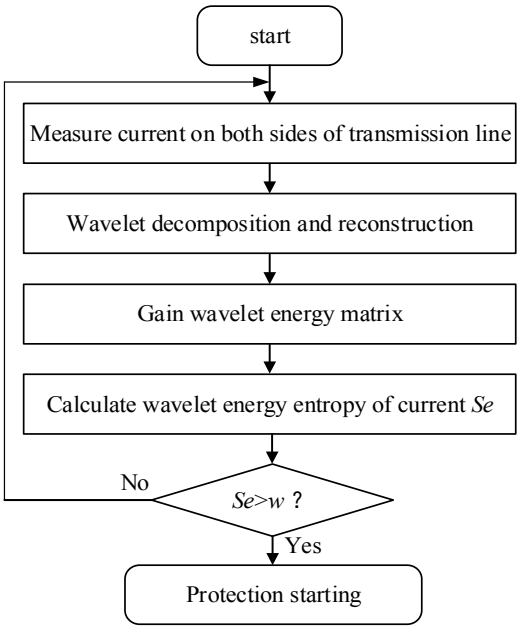

Figure 6. Flowchart of protection start-up based on wavelet energy entropy.

4.2. Protection Criterion

Based on analysis of the direction features of voltage and current measured on both sides of a HVDC transmission line, the relative entropy of wavelet energy is used as protection criterion to discriminate between internal faults and external faults. For internal faults, the direction of the voltage component and the direction of the current component at the rectifier-side are opposite, while the direction of the voltage component and the direction of the current component at the inverter-side are identical, so that the relative entropy of the wavelet energy of voltage fault components and current fault components at the rectifier-side is much larger than that at the inverter-side. Let M_R be the relative wavelet energy entropy of a voltage fault component and current fault component at the rectifier-side, and M_I be the

relative wavelet energy entropy of a voltage fault component and current fault component at the inverter-side. Therefore, the protection criterion for internal and external faults is formulated as follows:

$$\begin{cases} \dfrac{M_R}{M_I} > \varepsilon \ \text{ Internal fault,} \\ \dfrac{M_R}{M_I} \le \varepsilon \ \text{ External fault,} \end{cases} \tag{22}$$

where ε is the threshold that distinguishes internal faults from external faults.

The method utilizes the direction of fault components of voltage and current when the control system fails to operate or adjust to a steady state. That is to say, the voltage and current measured by the protector haven't changed yet. The fault components of voltage and current should be computed after decoupling. We analyze the fault components of voltage and current by WT, where the "dB4" mother wavelet and 10-scaled WT are chosen in the transformation. The energy of components on each level after wavelet transform is normalized. Then the relative wavelet energy entropy is calculated. The flowchart of the protection method using relative wavelet energy entropy is shown in Figure 7.

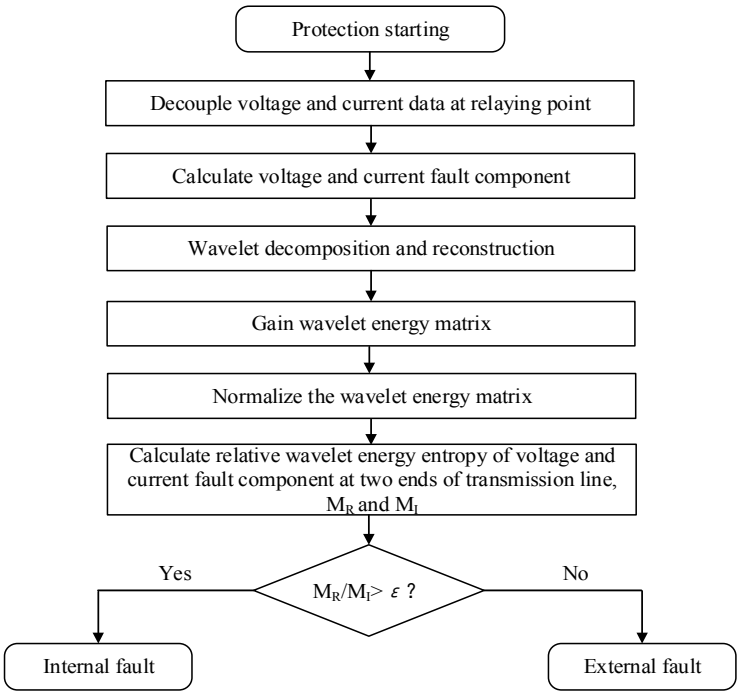

Figure 7. Flowchart of the pilot protection scheme based on relative entropy of wavelet energy.

5. Simulation and Discussion

A bipolar HVDC system is built for simulation in PSCAD/EMTDC. The power system is ±800 kV and rated current is 4 kA. Its transmission capacity is 6400 MW. Figure 1 shows a general structure sketch of the HVDC transmission system with two 1500-km-long transmission lines which adopts six-splitting lead of JMarti model. Smoothing reactor is 400 mH, and a 12/24/36 three tuning DC filter is adopted in the HVDC system model.

Let fault distance be the distance between the fault point and the relaying point, and the setting sampling frequency is 100 kHz. The time window of the protection initiation criterion is 0.2 ms (that is 20 sampling points), while the time window of the protection criterion is 5 ms (that is 500 sampling points). Moreover, according to our analysis of simulations under various kinds of fault conditions, the threshold of starting criterion w is 7×10^{-4}, while the threshold of protection criterion ε is set to 3.

In this section, the starting criterion and protection criterion based on wavelet entropy of current and voltage are used for fault detection and HVDC transmission line protection. The following strategy is carried out according to the schemes in Figures 6 and 7. Signals are acquired by simulation of the system in Figure 1.

In order to evaluate the proposed method, the main characteristics concerning wavelet energy entropy and relative wavelet energy entropy, which are assessed in the frequency domain and time domain via wavelet transform, are discussed. For instance, monopole grounding faults, two-pole faults and different kinds of external fault are simulated with different resistance faults. Then, wavelet energy entropy is applied using a sliding window with length of 20 samples. Figures 8–10 show the obtained results for fault detection. Figure 8 shows the transient behavior of current at rectifier-side, and the wavelet energy entropy computation under positive polar grounding fault with fault resistance R_f = 0.1Ω and fault distance at 100 km.

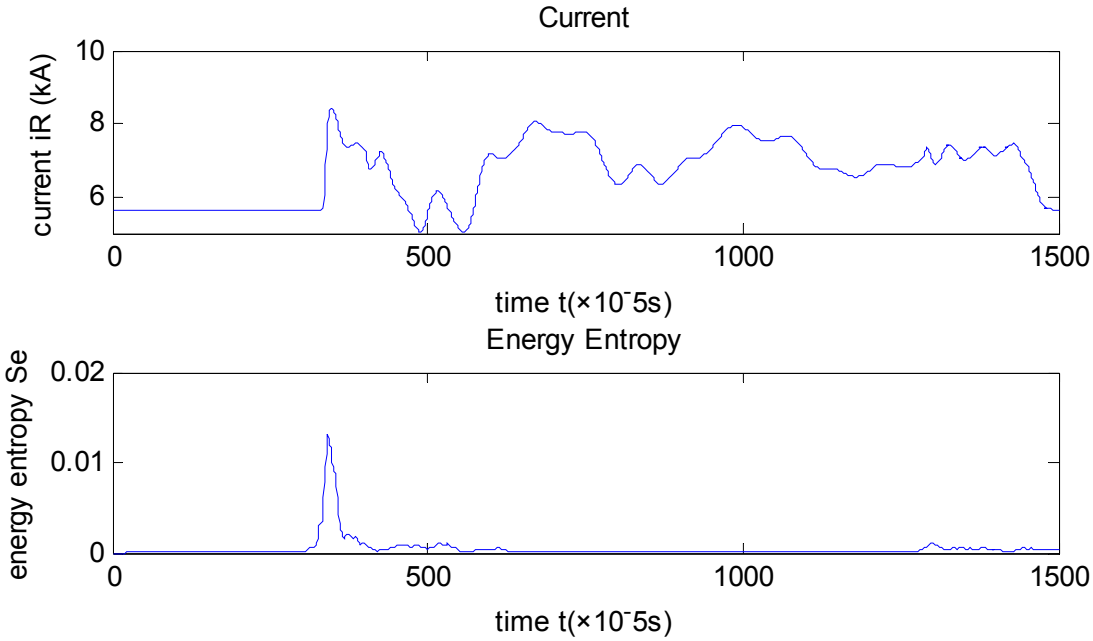

Figure 8. Transient behavior of current signal measured at rectifier-side of energy entropy under monopole fault with fault resistance R_f = 0.1 Ω and fault distance at 100 km.

Figure 9 depicts results for a two-pole fault with fault resistance R_f = 100 and fault distance at 400 km. Figure 10 illustrates results for an external fault at the rectifier-side. Results show clearly the detection time for all fault types that are tested. Thus, the proposed starting criterion only uses the wavelet energy entropy of the currents, concluding that the starting criterion is an effective algorithm for fault detection and protection startup, since the WEE detects any fault type reliably and rapidly and improves the detection time under fault conditions.

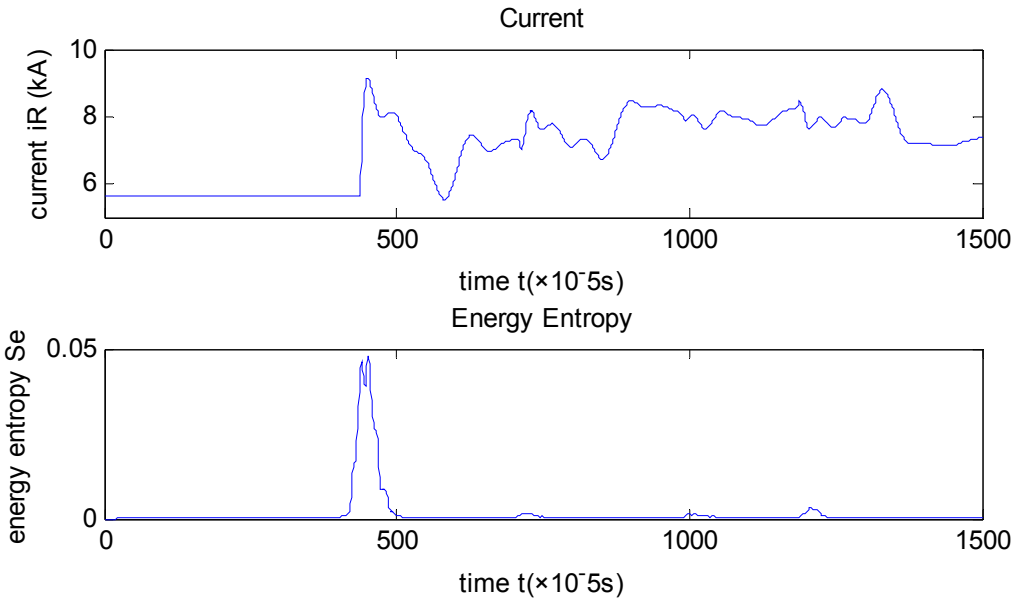

Figure 9. Transient behavior of current signal measured at rectifier-side of energy entropy under two-pole fault with fault resistance R_f = 100 Ω and fault distance at 400 km.

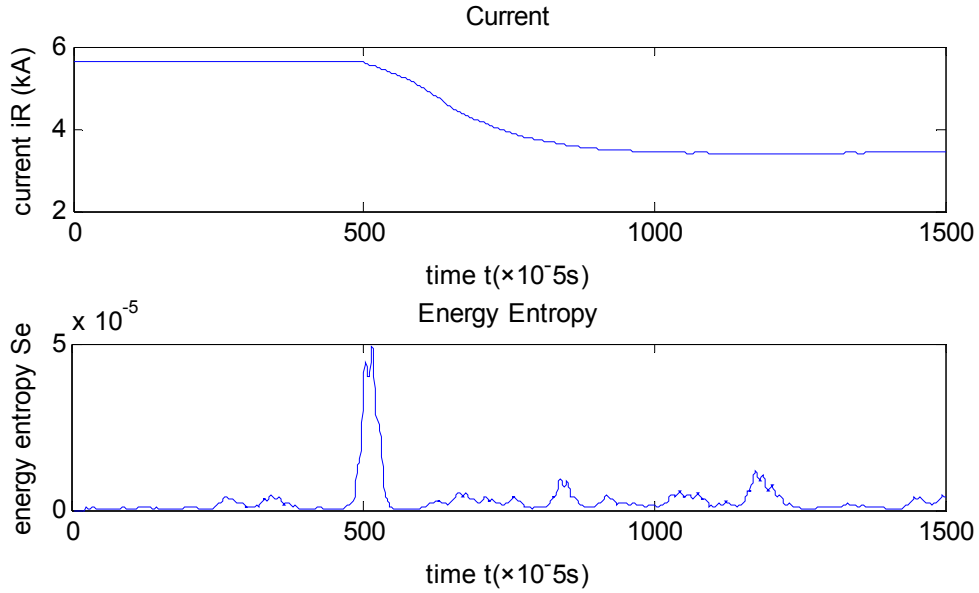

Figure 10. Transient behavior of current signal measured at rectifier-side of energy entropy under external fault at inverter-side.

The starting criterion is carried out via energy entropy while the protection criterion is carried out via relative entropy of wavelet energy, and it is extensively assessed by simulations using multiple cases. These cases are simulated at the same inception time 0.35 s while varying in fault distance, fault impedance for each fault and noise level for each signal.

Simulations are conducted under the conditions that fault occurs at 0.35 s and fault distances of 1, 100, 750, 1490, and 1499 km for different types of fault with signal-noise ratio of 30 dB. The starting criterion realizes fault detection and determine the inception time of fault diagnosis. Table 1 displays the results of fault diagnosis considering the fault distance, fault resistance, fault types and noise level.

Table 1. Inception time of different types of fault determined by the starting criterion.

Fault position		Inception time (s)	
		Current measured at R I_r	Current measured at I I_i
F1	1km	0.34846	0.35505
	750km	0.34999	0.35248
	1499km	0.35505	0.34975
F2	1km	0.35007	0.35505
	750km	0.35249	0.35199
	1499km	0.35504	0.34737
F3	1km	0.34796	0.35490
	750km	0.34839	0.35242
	1499km	0.35194	0.34978
F4	Rectifier-side	0.35245	0.35840
	Inverter-side	0.34861	0.35182
F5	A phase grounding fault at rectifier-side	0.35185	0.35889
	A phase grounding fault at inverter-side	0.35104	0.35018

Besides, fault resistances of 0.1, 100, and 1000 Ω for different types of fault with signal-noise ratio of 30 dB are simulated. The increasing values of grounding resistance indicate the decline of current, but the abovementioned feature doesn't change so the protection system can still start.

To classify a detected fault, a 5 ms time window after detection is used for computing the relative wavelet energy entropy. For instance, in Table 2 the results of different kinds of fault conditions with different fault distances are presented. Protection is carried out using the procedure summarized in Figure 7. If a monopole grounding fault occurs at 1 km (when its fault resistance is 0Ω), the wavelet energy relative entropy of voltage and current fault component at the rectifier-side is 0.1415, and that at the inverter-side it is 2.775×10^{-3}. These computations are used to follow the protection principle and it can be seen that $M_R / M_I > \varepsilon$, so an internal fault took place and the protection relay should operate. The same process is followed for each simulation case. Table 3 displays the results of different kinds of fault conditions with a noise level of 30 dB. In accordance to the attained results the relative entropy of wavelet energy can recognize internal fault regardless of fault position, fault resistance and noise level.

Table 2. Results for different fault types with different fault positions (no noise).

Fault position	Fault distance	M_R	M_I	M_R/M_I	Result
F1	1	0.1415	2.775×10^{-3}	50.99	1
	100	0.1154	4.426×10^{-3}	15.22	1
	750	8.689×10^{-3}	9.68×10^{-4}	21.0730	1
	1490	2.81×10^{-2}	5.049×10^{-3}	5.565	1
	1499	4.774×10^{-2}	1.37×10^{-2}	3.485	1
F2	1	0.1978	4.784×10^{-3}	41.35	1
	100	0.1036	4.066×10^{-3}	25.48	1
	750	8.503×10^{-3}	8.691×10^{-4}	9.784	1
	1490	2.854×10^{-2}	4.681×10^{-3}	6.097	1
	1499	4.911×10^{-2}	1.311×10^{-2}	3.746	1

Table 2. *Cont.*

Fault position	Fault distance	M_R	M_I	M_R/M_I	Result
F3	1	0.1672	5.442×10^{-3}	30.72	1
	100	8.187×10^{-2}	4.899×10^{-3}	16.72	1
	750	2.541×10^{-2}	4.359×10^{-4}	58.28	1
	1490	3.272×10^{-2}	4.063×10^{-4}	80.53	1
	1499	1.196×10^{-3}	7.27×10^{-5}	16.45	1
F4: Rectifier-side	-	9.18×10^{-5}	1.098×10^{-2}	8.361×10^{-3}	0
F4: Inverter-side	-	1.189×10^{-2}	8.821×10^{-3}	1.348	0
F5: A phase grounding fault at rectifier-side	-	3.334×10^{-3}	2.196×10^{-3}	1.518	0
F5: A phase grounding fault at inverter-side	-	3.695×10^{-4}	8.847×10^{-3}	4.177×10^{-2}	0

Result "1" represents that internal fault occurs and the protection relay operates, while "0" is an indicator of protection system reset. Similarly hereinafter.

Table 3. Results for different fault types with different fault positions (when noise level is 30dB).

Fault position	Fault distance	M_R	M_I	M_R/M_I	Result
F1	1	0.2862	1.924×10^{-3}	148.8	1
	100	0.201	8.089×10^{-3}	24.85	1
	750	6.591×10^{-2}	1.998×10^{-3}	32.99	1
	1490	9.689×10^{-2}	2.289×10^{-2}	4.233	1
	1499	4.352×10^{-2}	1.077×10^{-2}	4.041	1
F2	1	0.2658	9.927×10^{-3}	26.78	1
	100	0.2778	1.837×10^{-2}	15.12	1
	750	8.811×10^{-2}	3.234×10^{-3}	27.24	1
	1490	3.452×10^{-2}	8.516×10^{-3}	4.0535	1
	1499	2.587×10^{-2}	7.54×10^{-3}	3.431	1
F3	1	0.3986	7.863×10^{-3}	50.69	1
	100	0.1421	1.251×10^{-2}	11.36	1
	750	5.593×10^{-2}	2.768×10^{-4}	556.5	1
	1490	4.011×10^{-2}	9.645×10^{-3}	4.159	1
	1499	6.458×10^{-2}	2.258×10^{-3}	28.6	1
F4: Rectifier-side	-	1.506×10^{-2}	1.743×10^{-2}	0.8640	0
F4: Inverter-side	-	3.895×10^{-2}	8.371×10^{-2}	0.4653	0
F5: A phase grounding fault at rectifier-side	-	6.685×10^{-3}	3.885×10^{-3}	1.721	0
F5: A phase grounding fault at inverter-side	-	5.549×10^{-2}	8.427×10^{-2}	0.6585	0

Table 4. Results for internal fault with different fault resistance.

Fault position	Fault resistance	M_R	M_I	M_R/M_I	Result
F1 100 km	0.1	0.1154	4.426×10^{-3}	26.07	1
	100	0.1008	6.281×10^{-3}	16.05	1
	1000	0.1059	5.8×10^{-3}	18.26	1
F2 750 km	0.1	8.503×10^{-3}	8.691×10^{-4}	9.784	1
	100	7.74×10^{-3}	7.247×10^{-4}	10.68	1
	1000	1.193×10^{-2}	8.587×10^{-6}	1389	1
F3 1499 km	0.1	1.196×10^{-3}	7.27×10^{-5}	16.45	1
	100	3.952×10^{-2}	4.126×10^{-3}	9.578	1
	1000	3.184×10^{-2}	9.997×10^{-3}	3.185	1

6. Conclusions

A pilot protection method for HVDC transmission lines by using the directional features of voltage fault components and current fault components is presented in this paper. According to this method, the directions of voltage and current fault components measured at both sides is extracted with the relative wavelet energy entropy. The ratio of relative entropy of voltage and current fault components on two ends of the line in an internal fault differs obviously from that under external fault conditions. Thus we can discriminate between internal faults and external faults. In the proposed method, only voltage and current information is used with a time window of 5 ms, and it doesn't require synchronous sampling on both ends of the line, so the communication channel demands can be easily satisfied. A simulation model is established on the PSCAD/EMTDC platform for a HVDC transmission line system with a rated voltage of 800 kV and line length of 1500 km. According to our theoretical analysis and simulation results, the proposed method is proved to be adaptable for different fault locations, fault types, fault resistance, and under noise conditions.

Acknowledgments

This work is supported by National Natural Science Foundation of China (No. 51307145), and the Application Basic Research Project of Sichuan Province (No. 2014JY0177).

Author Contributions

All authors have read and approved the final manuscript.

Conflicts of Interest

The authors declare no conflict of interest.

References

1. Song, G.; Chu, X.; Gao, S.; Kang, X.; Jiao, Z. A new whole-line quick-action protection principle for HVDC transmission lines using one-end current. *IEEE Trans. Power Deliv.* **2015**, *30*, 599–607.

2. Schmidt, G.; Fiegl, B.; Kolbeck, S. HVDC transmission and the environment. *Power Eng. J.* **1996**, *10*, 204–210.
3. Anderson, P.M. *Power System Protection*; McGraw-Hill: New York, NY, USA, 1999; pp. 915–955
4. Long, W.; Nilsson, S. HVDC transmission: Yesterday and Today. *Power Energy Mag.* **2007**, *5*, 22–31.
5. Kong, F.; Hao, Z.; Zhang, S.; Zhang, B. Development of a novel protection device for bipolar HVDC transmission lines. *IEEE Trans. Power Deliv.* **2014**, *29*, 2270–2278.
6. Liu, J.; Fan, C.; Tai, N. A novel pilot directional protection scheme for HVDC transmission line based on specific frequency current. In Proceedings of the 2014 International Conference on Power System Technology (POWERCON 2014), Chengdu, China, 20–22 October 2014; pp. 976–982.
7. Xing, L.; Chen, Q.; Gao, Z. A new protection principle for HVDC transmission lines based on directions of fault components of voltage and current. *Autom. Electr. Power Syst.* **2013**, *37*, 107–113. (in Chinese)
8. Li, Z.; Lv, Y. A novel scheme of HVDC transmission line voltage traveling wave protection based on wavelet transform. In Proceedings of the 2008 International Conference on High Voltage Engineering and Application, Chongqing, China, 9–13 November 2008; pp. 163–167.
9. He, Z.; Lin, S.; Deng, Y.; Li, X.; Qian, Q. A rough membership neural network approach for fault classification in transmission lines. *Int. J. Electr. Power Energy Syst.* **2014**, *61*, 429–439.
10. Aguilar, R.; Pérez, F.; Orduña, E.; Rehtanz, C. The directional feature of current transients, application in high-speed transmission-line protection. *IEEE Trans. Power Deliv.* **2013**, *28*, 1175–1182.
11. Dubey, R.; Samantaray, S.R. Wavelet singular entropy-based symmetrical fault-detection and out-of-step protection during power swing. *Gener. Transm. Distrib.* **2013**, *7*, 1123–1134.
12. Fu, L.; He, Z.Y.; Bo, Z.Q. Wavelet transform and approximate entropy based identification of faults in power swings. In Proceedings of the IET 9th International Conference on Developments in Power System Protection 2008, Glasgow, UK, 17–20 March 2008; pp. 590–594.
13. Fu, L.; He, Z.Y.; Mai, R.K.; Bo, Z.Q. Approximate entropy and its application to fault detection and identification in power swing. In Proceedings of the IEEE Power & Energy Society General Meeting 2009, Calgary, AB, USA, 26–30 July 2009; doi:10.1109/PES.2009.5275380.
14. Liu, Q.; Wang, Z. Study on non-unit transient protection principle for EHV transmission lines based on wavelet singular entropy. In Proceedings of the IEEE Power & Energy Society General Meeting, 2009, Calgary, AB, Canada, July. 26–30, 2009; doi:10.1109/PES.2009.5275613.
15. He, Z.; Fu, L.; Lin, S.; Bo, Z. Fault detection and classification in EHV transmission line based on wavelet singular entropy. *IEEE Trans. Power Deliv.* **2010**, *25*, 2156–1163.
16. Yang, M.Y.; Yang, Y.K. A study of transient-based protection using wavelet energy entropy for power system EHV transmission line. In Proceedings of the 2010 International Conference on Wavelet Analysis and Pattern Recognition, Qingdao, China, 11–14 July 2010; pp. 283–288.
17. Seryasat, O.R.; Aliyari shoorehdeli, M.; Honarvar, F. Multi-fault diagnosis of ball bearing using FFT, wavelet energy entropy mean and root mean square (RMS). In Proceedings of the 2010 IEEE International Conference on Systems Man and Cybernetics (SMC), Istanbul, Turkey, 10–13 October 2010; pp. 4295–4299.

18. Schmitt, H.L.; Silva, R.B.; Scalassara, P.R.; Goedtel, A. Bearing fault detection using relative entropy of wavelet components and artificial neural networks. In Proceedings of the 2013 9th IEEE International Symposium on Diagnostics for Electric Machines, Power Electronics and Drives (SDEMPED), Valencia, Spain, 27–30 August 2013; pp. 538–543.